Optical Multipath Interference Mitigation for PAM4 Transmission Using Line Coding and High-pass Filtering

Ning Cheng[1], Dechao Zhang[2], Dawei Ge[2], Yan Song[1], Meijuan Lv[1], Shanglin Li[1], Bin Lv[1] and Xuezhe Zheng[1]
[1] Innolight Technologies, 168 Shengpu Road, Suzhou, Jiangsu, China
[2] Department of Fundamental Network Technology, China Mobile Research Institute, Beijing, China 100053.
ning.cheng@innolight.com

Abstract: A simple method using DC-balanced line-coding and receiver-side high-pass filtering is proposed to mitigate MPI in high-speed PAM4 transmission. 5-dB improvement in MPI tolerance is achieved in both simulations and experiments for 25GBd PAM4 transmissions.

1. Introduction

Advanced modulation formats with intensity modulation and direct detection (IM/DD), such as pulse amplitude modulation and carrier-less amplitude and phase modulation, provide a cost-efficient way to improve the capacity of short-reach fiber-optic communication systems. In particular, 4-level pulse amplitude modulation (PAM4) has wide applications in data centers and mobile front-hauls [1, 2] due to its low complexity, small footprint, low cost, and small power consumption. However, previous studies have shown that compared to the NRZ scheme, PAM4 transmission is more susceptible to optical multipath interference (MPI) [3]. In fiber optic transmission links, there exist multiple reflections from transmitters, fiber connectors, and receivers. These reflections create delayed and attenuated versions of the transmitted signal with random polarization and phase. When the direct pass-through signal and even-order multipath reflections are combined and detected by a photodiode at the receiver, the interferometric effect converts the laser phase noise to intensity noise degrading the transmission performance [4]. To mitigate the detrimental impact of MPI on PAM4 transmission, various schemes have been proposed using digital filters at the receiver side [5, 6]. Because of the low-frequency nature of the MPI noise, these digital filters use a large number of taps or a burdensome FFT size, resulting in relatively complex digital signal processing and significant power consumption. Alternatively, a simple high-pass filter can be utilized at the receiver side to filter out a large portion of the MPI noise [7]. Such an approach is relatively easy to implement, but the improvement in MPI tolerance is very limited (~2 dB) when the transmitted signal has a moderate frequency chirp [7]. Furthermore, the high-pass filtering leads to baseline wander in the received signal and hinders data recovery [5]. Long baseline wander could introduce consecutive symbol errors and make forward error correction less effective.

This paper proposes a simple method to mitigate the optical MPI in high-speed PAM4 transmission, using DC-balanced line coding and receiver-side high-pass filtering. Both simulations and experiments on 25GBd PAM4 transmission demonstrate 5-dB improvement in MPI tolerance using either 8B10B or MB810 line coding and a simple high-pass filter at the receiver. Furthermore, this paper presents a simple approach to encode a DC-balanced PAM4 signal from an 8B10B or MB810 binary line code. A practical method to measure the MPI noise spectrum using short pseudo-random bit sequence (PRBS) patterns is also demonstrated, providing a better understanding of the MPI noise generated from a PAM4 signal with frequency chirp.

2. DC-balanced line coding for MPI mitigation

The proposed method for MPI mitigation is illustrated in Fig. 1(a). In this approach, a DC-balanced PAM4 line coding is implemented, and a high-pass analog filter (HPF) is used at the receiver. The HPF can be a simple 1st-order RC filter or a 4th-order Bessel filter with linear phase response. In the following, a 4th-order Bessel filter is used in the simulations, and a

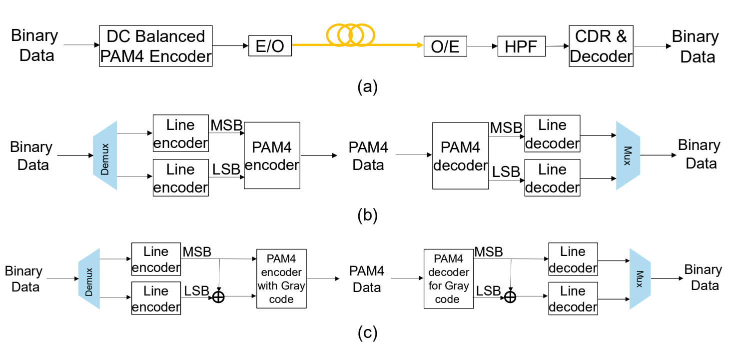

Fig. 1 DC-balanced PAM4 line coding and high-pass filtering for MPI mitigation.

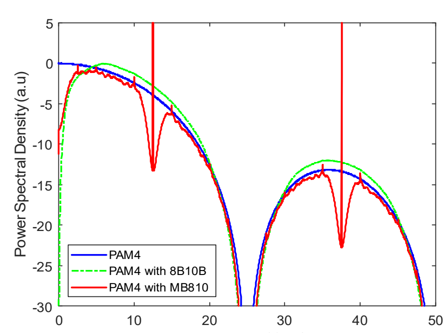

Fig. 2 Power spectral density of PAM4 signals.

1st-order RC filter is implemented in the experiments due to its simple structure. It is worth mentioning that both filters can effectively remove a large portion of the MPI noise and improve the MPI tolerance in PAM4 transmission. DC-balanced line coding, such as 8B10B, MB810 and 27S/32S line codes [8], alleviates DC wandering after the high-pass filter. Due to its simplicity and wide-spread use in Ethernet, 8B10B line code is used in our study, as well as MB810 line code whose spectrum is bounded within the Nyquist band [9]. 8B10B (or MB810) code is originally designed for DC-balanced binary line signaling. Special care must be taken to ensure DC-balance is maintained after PAM4 encoding. As shown in Fig. 1(b), the binary data stream is first demultiplexed into odd and even bit sequences. Then these bit sequences are separately encoded using 8B10B (or MB810) line code. Finally, the PAM4 encoding is done by taking these two 8B10B (or MB810) bit sequences as the MSB (most significant bit) and LSB (least significant bit), respectively. Since Gray code is commonly used for PAM4 signaling, additional XOR operation must be performed on the encoded bit sequences, as shown in Fig. 1(c). Fig. 2 shows the simulated power spectral density of the PAM4 signal using the encoding scheme shown in Fig. 1(b). Around zero frequency, the power spectral density is very low with 8B10B or MB810 encoding, and hence this simple coding scheme is able to achieve DC-balanced PAM4 signaling. In comparison, without the help of the demultiplexer, we directly encode the original binary data by 8B10B (or MB810) and then subsequently encode the DC-balanced binary bit sequence into the corresponding PAM4 signal. In this case, the deep spectral null at zero frequency disappears as shown by the blue curve in Fig. 2, because PAM4 encoding destroys the DC balance of the original 8B10B (or MB810) binary sequence.

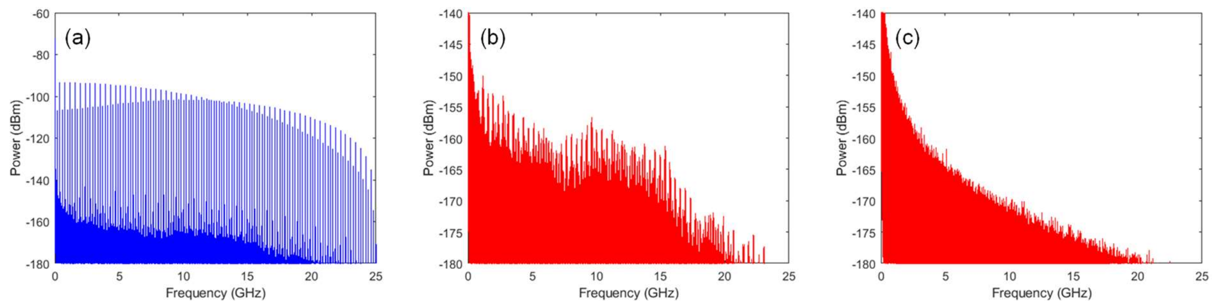

Fig. 3 Power spectral density with −30-dB effective MPI

3. MPI noise characterization

To mitigate the impact of the MPI noise in PAM4 transmission, it is necessary to understand the MPI noise spectrum. When a CW (continuous-wave) laser output transmits through a fiber link, MPI is introduced due to multiple reflections in the link. The MPI noise spectrum was found concentrating at low frequencies [4]. In real systems, the PAM4 signal is generated by optical carrier modulation, causing the modulated signal has a much broader spectrum than an unmodulated CW carrier. In addition, the frequency chirp introduced by an optical modulator further broadens the signal spectrum [7]. Under large signal modulation, it is difficult to analyze or measure the MPI noise, considering that the MPI noise is mixed with the modulated signal at the receiver. To the author's knowledge, there is no efficient way to analyze or measure MPI noise in PAM4 transmission yet. Here we propose a practical approach to measure the MPI noise spectrum under large signal modulation. At the transmitter side, the CW carrier is modulated by a PRBS pattern with a short sequence length L_{PRBS}, for example, using a PRBS 2^7-1 pattern. Because the short PRBS pattern is repeated periodically in time domain, the modulated signal has a discrete line spectrum on frequencies at $N/(L_{PRBS}\cdot T_S)$, where $N = 0, 1, 2, 3, \ldots$, and T_S is the symbol period. In contrast, the MPI noise, generated by the interference between the transmitted signal and the reflections, exhibits a continuous spectrum. The spectrum of the received signal includes the discrete line spectrum from the signal and the continuous spectrum from MPI noise, as shown in Fig. 3(a). With the removal of the line spectrum at frequencies $N/(L_{PRBS}\cdot T_S)$, the continuous MPI noise spectrum is revealed at frequencies other than $N/(L_{PRBS}\cdot T_S)$. To recover the spectrum information of the MPI noise at frequencies $N/(L_{PRBS}\cdot T_S)$, a different PRBS pattern length, L'_{PRBS}, is utilized to conduct the same procedure. Using this approach, we were able to obtain the continuous MPI noise spectrum generated from a 25GBd PAM4 signal using an electro-absorption modulated laser (EML), and the result is shown in Fig. 3(b). In comparison, Fig. 3(c) is the measured MPI noise spectrum when a CW carrier transmits through the same fiber link. From these measurement, it is clear that (i) MPI noise has most of its energy concentrating at low frequencies; and (ii) MPI noise from the modulated signal has more energy at higher frequencies because the modulated signal has a much broader spectrum due to the optical modulation and the frequency chirp introduced by the optical modulator. The MPI noise spectrum provides valuable information for designing an optimal filter at the receiver, as explained in the following section.

4. MPI noise mitigation

To verify the proposed MPI mitigation method, 25GBd PAM4 transmission is performed using the setup shown in Fig. 4.

At the transmitter side, a DC-balanced PAM4 signal with a PRBS pattern length of 2^{21} is used to modulate a 1310-nm optical carrier using an 18-GHz EML. To emulate the MPI generated in a real fiber link, the transmitted signal is split into two paths: the signal path and the MPI path. These two paths have a 10-km length difference, much longer than the optical carrier's coherence length (< 100 m). A variable attenuator in the MPI path controls the effective MPI level. Before the optical receiver, signals from the two paths are combined to generate MPI. In the simulations, the polarization of the MPI signal is intentionally aligned with the PAM4 signal to evaluate the worst impact of MPI noise. To emulate a more practical fiber link, a polarization scrambler is used in the experiments. After the optical signal is detected by a 15-GHz receiver optical subassembly (ROSA), a high-pass filter with a variable cutoff frequency from 5MHz to 150MHz is used for filtering out the MPI noise. The optimal filter bandwidth can be determined from the measured signal and MPI noise spectrum, by maximizing the signal-to-noise ratio. A decision circuit at the receiver recovers the PAM4 symbols, and binary data are decoded from the PAM4 symbols. The bit error rate (BER) curves are measured by comparing the transmitted and recovered binary bit sequences. The receiver sensitivity at the KP4 FEC threshold (BER = 2.4×10^{-4}) is calculated from the BER curves. Comparing the receiver sensitivities with and without MPI, the power penalty values are calculated for different MPI levels. The simulation and experimental results for the MPI penalty are presented in Fig. 5. In the simulations, MPI introduces significant power penalties for conventional 25GBd PAM4 transmission (i.e., without line coding and high-pass filtering) when the effective MPI is larger than –32 dB. With our proposed approach using DC-balanced 8B10B (or MB810) encoding and receiver-side high-pass filtering, the MPI penalty remains less than 1 dB for effective MPI as high as –27 dB. Different high-pass filters, 4th-order Bessel filter (HPF1) and 1st-order Butterworth filter (HPF2), with optimal cutoff frequency result in slightly different MPI tolerances. In view of the line coding overhead of 8B10B or MB810, symbol rate must be increased by 25% to achieve the same net payload. Fig. 5(a) also shows the simulation results for 30GBd PAM4 transmission using DC-balanced MB810 encoding and high-pass filtering. Increasing the symbol rate from 25 to 30GBd leads to a slight degradation in receiver sensitivity. However, with our proposed approach, we can still achieve 5-dB improvement in MPI tolerance even with the increased symbol rate. Fig. 5(b) shows the experimental results for power penalties induced by different MPI levels. With conventional 25GBd PAM4, MPI noise introduces more than 1-dB power penalty when the effective MPI is higher than –30 dB. In comparison, the simulation results in Fig. 5(a) showed a 1-dB power penalty at –32-dB MPI for conventional 25GBd PAM4. The discrepancy of 2dB results from the aligned MPI polarization in the simulations and the scrambled MPI polarization in the experiments. When 8B10B (or MB810) encoding and high-pass filtering are implemented in a QSFP28 module, the MPI tolerance is improved by 6 dB in our experiments, as shown in Fig. 5(b). Both the simulations and experiments proved the effectiveness of our proposed method for MPI mitigation.

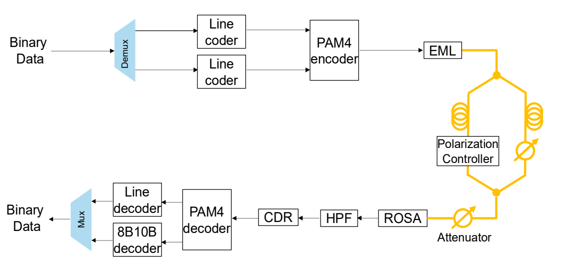

Fig. 4 Experimental setup for PAM4 transmission with MPI.

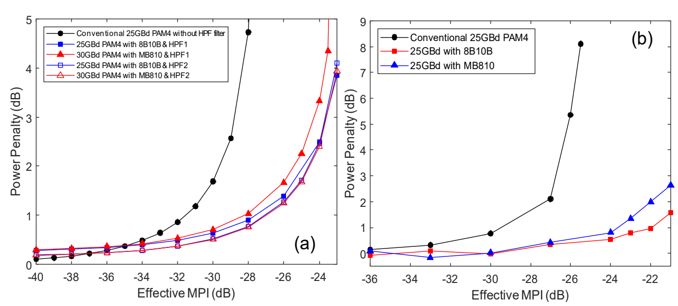

Fig. 5 Power penalty induced by MPI noise

5. Conclusions

In summary, we demonstrated a simple yet effective approach to mitigate the MPI impact in high-speed PAM4 transmission. Simulations and experiments showed a 5-dB improvement using this method. In addition, the MPI noise spectrum generated from the modulated optical signal was measured using short PRBS patterns. The results revealed that for PAM4 signals with significant frequency chirp, MPI noise power spreads to higher frequencies due to spectrum broadening.

6. References

[1] IEEE 802.3bs-2017, http://www.ieee802.org/3/bs/, and 100G Lambda MSA, http://100glambda.com/.

[2] N. Eiselt et al., "Performance comparison of 112-Gb/s DMT, Nyquist PAM4, and partial-response PAM4 for future 5G Ethernet-based fronthaul architecture," J. Lightwave Technol. **36**, pp. 1807–1814, 2018.

[3] C. R. S. Fludger et al., "Experimental measurements of the impact of multipath interference on PAM signals," OFC 2014, paper W1F.6.

[4] J. L. Gimlett and N. K. Cheung, "Effects of phase-to-intensity noise conversion by multiple reflections on gigabit-per-second DFB laser transmission systems," J. Lightwave Technol. **7**, pp. 888–895, 1989.

[5] C. Huang et al., "Optical multipath interference mitigation for high-speed PAM4 IMDD transmission system," JLT **40**, pp. 5490–5501, 2022.

[6] B. P. Smith, et al., "Circuit for multipath interference mitigation in an optical communication system," U.S. Patent, US9876581B2.

[7] Y. J. Wen et al., "Mitigation of optical multipath interference impact for directly detected PAMn system," Optics Express **28**, pp.38317–38332, 2020.

[8] M. Shekar et al., "A 27S/32S DC-balanced line coding scheme for PAM-4 signaling," International Conference on VLSI Design, pp.222–227, 2021.

[9] C. Lee et al., "A new line code for 10-Gigabit Ethernet: MB810," IEEE International Conference on Communications, pp.1774–1777, 2000.